

## PERFORMANCE OF FRICTION AND WEAR OF ELECTROSPARK DEPOSITED Ni-MoS<sub>2</sub> SELF-LUBRICATING COATING

C. GUO<sup>a,b</sup>, F. KONG<sup>a</sup>, S. ZHAO<sup>c</sup>, X. YAN<sup>d</sup>, J. YANG<sup>a,\*</sup>, J. ZHANG<sup>a</sup>

<sup>a</sup>*School of Equipment Engineering, Shenyang Ligong University, Shenyang 110159, China*

<sup>b</sup>*Chongqing Jianshe Industry (Group) LLC, Chongqing 400054, China*

<sup>c</sup>*Shandong Special Industry Group Co. Ltd, Zibo 255201, China*

<sup>d</sup>*North Huaan Industry Group Co. Ltd, Qiqihaer 161046, China*

A Ni-MoS<sub>2</sub> sintered composite was used as an electrode to prepare a coating on a CrNi3MoVA steel substrate by using electrospark deposition technique. The nanomechanical properties and friction and wear performance of the coating were tested by employing nanoindenter and friction and wear tester, and the morphologies, composition and phase structure were analyzed by utilizing scanning electron microscopy (SEM), energy dispersive X-ray spectrum (EDS) and X-ray diffraction(XRD). The results showed that the Ni-MoS<sub>2</sub> coating is composed of MoS<sub>2</sub>,  $\gamma$ -Ni, MoO<sub>2</sub> and Ni<sub>x</sub>S as the electrode reacted with the mixing O<sub>2</sub> in the ESD process. The coating exhibits excellent tribological properties for its friction coefficient reduced about 75% and its wear resistance increased about 77% in contrast to the CrNi3MoVA steel.

(Received April 29, 2019; Accepted July 1, 2019)

*Keywords:* Self-lubricating coating, Electrospark deposition, Ni-MoS<sub>2</sub>, Friction and wear

### 1. Introduction

Surface wear can lead to premature failure of a component, and then improper working of a device. The wear causes enormous economic loss with 1-2% of gross domestic product in a highly industrialized countries, so it is particularly significant to improve friction and wear performance of key component materials. Solid lubricants, which provide lubrication under essentially dry conditions, can be applied to mechanical components. MoS<sub>2</sub> is one of the most used solid lubricants worldwide by now, and its mechanism of functioning is based on its lamellar crystalline structure, in which the sulphur lamellae are bonded weakly with low shear strength. Although MoS<sub>2</sub> exhibits outstanding tribological properties, its friction coefficient and wear loss will increase rapidly in moist atmosphere due to the transformation of MoS<sub>2</sub> to MoO<sub>3</sub> which then breaks layer movement [1]. However, Self-lubricating composites containing MoS<sub>2</sub> and metal can possess excellent tribological properties in atmosphere.

Coating technology has been most widely applied to improve surface properties of a component made of metal [2-4]. The electrospark deposition (ESD) is a surface technique to prepare metallurgical bonded coatings with outstanding properties on metallic substrate materials. In an ESD process, the electrode (anode) and the substrate (cathode) are instantaneously tripped and discharged, and then the physical and chemical reactions take place in a micro melting pool on the surface of the substrate. The electrode moves back and forth on the contacting surface of the substrate, and the numerous micro melting pools link and overlap to form an ESD coating. Since ESD is a simple, cost-effective and environment-friendly technique applied in many industrial fields, great attention has been given to the research of coatings prepared by this technique. The recent researches about ESD technique showed that AlCoCrFiNi high-entropy alloy coatings [5],

---

\*Corresponding author: 373055507@qq.com

Zr-based amorphous-nanocrystalline coatings [6], Mo-Si-B coatings [7] and Cr-Al-Si-B coatings [8] can notably improve the tribological properties of alloy substrate.

Recently T. Cao, et al. [9] studied the friction and wear behavior of the Cu/Cu-MoS<sub>2</sub> self-lubricating coatings prepared by ESD, showing that the coatings have better wear resistance and lower friction coefficient than the high speed steel substrate, which indicates that the self-lubricating coating containing MoS<sub>2</sub> made by ESD has a wide application prospect. In this work, the friction and wear performance of a Ni-MoS<sub>2</sub> self-lubricating coating by ESD on a CrNi3MoVA steel substrate will be investigated.

## 2. Materials and methods

The CrNi3MoVA steel was used as substrate material and its chemical composition is shown in table 1. A bar of CrNi3MoVA steel was cut into rectangle-shape samples with a size of 20 mm×10 mm×5 mm by wire cutting. The nickel matrix self-lubricating composite (hereafter abbreviated as Ni-MoS<sub>2</sub>) was prepared by spark plasma sintering (SPS) using a mixture of argon-atomized nickel powder (50 wt%) and MoS<sub>2</sub> powder (50 wt%). The average particle size of Ni and MoS<sub>2</sub> was about 2 μm, and the purity was more than 99.9%. The mixed raw powders were filled in a graphite die and sintered in a KCE-FCT HP D 250-C furnace (Germany) under vacuum. The composite was heated from room temperature (RT) to 1100 °C at a heating rate of 50 °C/min, and then sintered at 1050 °C under the pressure of 40 MPa for 20 min, followed by furnace cooling. The bar of sintered Ni-MoS<sub>2</sub> composite was cut into cylinder-shape electrode with a size of Φ4 mm×50 mm by wire cutting. The samples and electrode were ground using SiC abrasive paper to an 800 grit finish, and then ultrasonically cleaned within ethanol and acetone mixture. The Ni-MoS<sub>2</sub> self-lubricating coating was prepared by using DJ-2000 type adjustable power metal surface repairing machine, and the optimized processing parameters through preliminary tests set as outlined in Table 2.

Table 1. Chemical composition of CrNi3MoVA steel [10].

C	Mn	Si	Cr	Ni	Mo	V	S	P
0.40	0.41	0.25	1.28	3.14	0.37	0.20	0.001	0.012

Table 2. Processing parameters of ESD.

Power/W	Ar gas flow/L·min <sup>-1</sup>	Electrode rotating rate/r·min <sup>-1</sup>	Deposition time unit area/min·cm <sup>-1</sup>
1200	12	3500	2.5

The hardness and elasticity modulus were tested by nano indentation G200 with Berkovich indenter and calculated by Oliver-pharr model through loading curves, and their values are the mean values of the eight parallel tested points in the middle of the coating in the thickness direction. The performance of friction and wear was tested by employing the MFT-5000 reciprocating friction and wear testing machine. Fig. 1 shows the schematic of friction and wear test. As shown in Fig. 1, the material of the grinding head is a quenched GCr15 steel ball with a diameter of 9.5 mm, the reciprocating distance 6 mm, the reciprocating speed 5 mm per second, the load 20 N and the total friction time 30 min. The worn mass of the samples was weighted by an electronic balance (Sartorius BP211D) with a sensitivity of 10<sup>-5</sup> g after ultrasonically cleaned within ethanol and acetone mixture for 60 min.

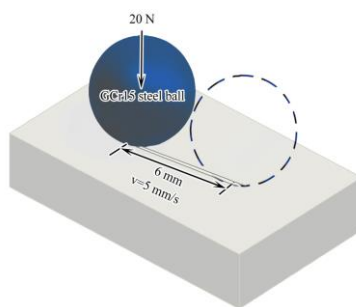


Fig. 1. Schematic of friction and wear test.

Original and worn morphologies were obtained by scanning electron microscopy (SEM, TESCAN MAIA3, Czech Republic), while the energy-dispersive spectrometer (EDS, X-Max, United Kingdom) was used to analyze the chemical composition of the selected-area. The phase constitution of the coating was identified by X-ray diffraction (XRD, X' Pert PRO, Holland).

### 3. Results and discussion

#### 3.1. Ni-MoS<sub>2</sub> coating microstructure

Fig. 2 shows the surface morphology (a) and EDS results of area A (b) of the Ni-MoS<sub>2</sub> coating. As shown in Fig. 2a, the surface morphology of the Ni-MoS<sub>2</sub> coating presents a splashing solidification feature by the plasma jet at high velocity. The EDS results of area A of the Ni-MoS<sub>2</sub> coating shown in Fig. 2b indicated that the coating has been oxidized although the ESD process is shielded by argon flow. Moreover, there is a small quantity of Fe in area A, indicative of elements diffusion from the substrate.

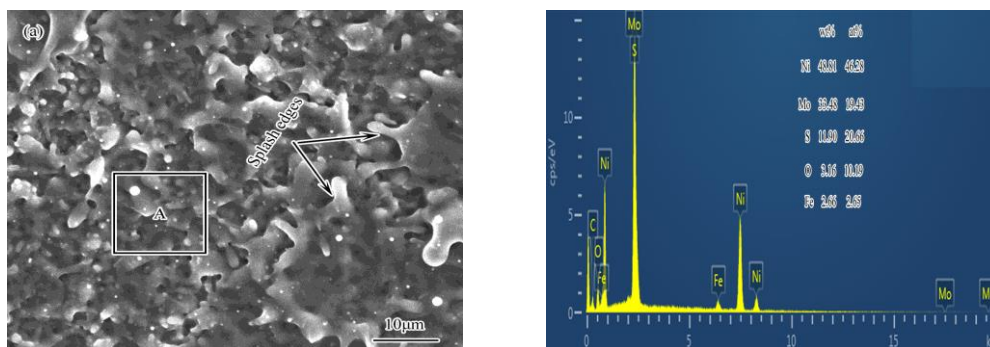


Fig. 2. Surface morphology (a) and EDS results of area A (b) of Ni-MoS<sub>2</sub> coating.

Fig. 3 shows the cross-section (a) morphology and EDS line scanning (b) of the Ni-MoS<sub>2</sub> coating. As shown in Fig. 3a, there is an obvious interface between the coating and the substrate for the steel substrate was etched by 4% Vol nital. The thickness of the coating is about 60 μm and its microstructure, free of cracks, is dense. The EDS line scanning of the Ni-MoS<sub>2</sub> coating (Fig. 3b) shows that there is a gradual transition region about 10 μm for Fe, indicating that Fe has diffused from the substrate to dilute into the coating, which forms a strong metallurgical bonding between the coating and the substrate.

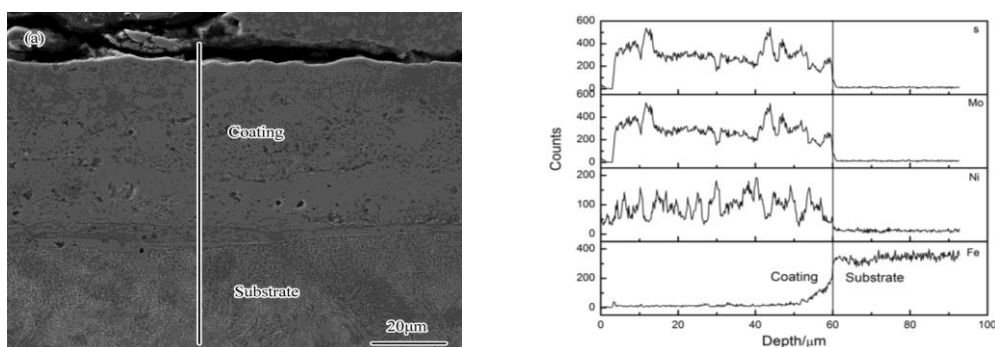


Fig. 3. Cross-section (a) morphology and EDS line scanning (b) of Ni-MoS<sub>2</sub> coating.

Fig. 4 shows the XRD pattern of the Ni-MoS<sub>2</sub> coating. As shown in Fig. 4, the Ni-MoS<sub>2</sub> coating is composed of MoS<sub>2</sub>, γ-Ni, MoO<sub>2</sub> and Ni<sub>x</sub>S. From the view of XRD pattern, peaks for NiS and Ni<sub>3</sub>S<sub>2</sub> are both detected, so Ni<sub>x</sub>S is used here. Based on the EDS and XRD results, there might be two kinds of reactions due to the mixing O<sub>2</sub> in the ESD process as follows:



In light of thermodynamic calculation [11], both the reactions have higher negative values of Gibbs free energies at high temperatures, which means these reactions could be favored in the ESD process. Noticeably, some amount of MoO<sub>2</sub> was in-situ formed in the coating by reacting with the mixing O<sub>2</sub>. The MoO<sub>2</sub> can act as an oxide dispersion strengthened (ODS) phase in the coating for it possesses a high melting point about 2600 °C and high hardness about HV1100 [12].

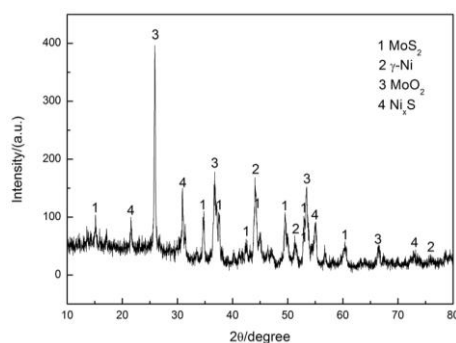


Fig. 4. XRD pattern of Ni-MoS<sub>2</sub> coating.

### 3.2. Nano-mechanical properties of CrNi3MoVA steel and Ni-MoS<sub>2</sub> coating

Table 3 shows the nano-mechanical properties of the CrNi3MoVA steel and the Ni-MoS<sub>2</sub> coating. As shown in Table 3, the hardness of the Ni-MoS<sub>2</sub> coating increases about 10.0%, and the elasticity modulus reduces about 46.2% than that of the CrNi3MoVA steel. Although MoS<sub>2</sub> has lower hardness, the Ni-MoS<sub>2</sub> coating still exhibits higher hardness than the CrNi3MoVA steel, which could possibly result from the following reasons. Firstly, the rapid melting and solidifying ESD process with a cooling speed of 10<sup>5</sup>-10<sup>6</sup> °C/s makes crystal nucleus difficult to grow, which brings about being tendency to form microscaled or even nanoscaled structure [13]. Secondly, the Fe diffused from the CrNi3MoVA steel (as shown in Fig. 1b) substrate to form solid solution in the coating. Thirdly, the presence of MoO<sub>2</sub> with higher hardness plays an important role to strengthen the coating.

Meanwhile, the other significant parameters to predict the serve life of the samples can also be obtained by the nanoindentation. The H/E value, relating to wear resistance of samples, determines the elasticity behavior limit of friction contacting surface. With the increase of the H/E value, the quantity of the asperity beyond the elasticity limit will reduce on the friction contacting surface under the stress, which enhances wear resistance due to reduced friction coefficient. As shown in Table 3, the H/E value of Ni-MoS<sub>2</sub> coating increases about 1.0 times than that of the CrNi3MoVA steel, which indicates that the Ni-MoS<sub>2</sub> coating has better wear resistance than the CrNi3MoVA steel. Moreover, the H<sup>3</sup>/E<sup>2</sup> value, another parameter relating to wear characteristic [14-15], represents the capability to resist plastic deformation under the contacting load, i.e. yield pressure. As shown in Table 3, the H<sup>3</sup>/E<sup>2</sup> value of the Ni-MoS<sub>2</sub> coating increases about 3.5 times than that of the CrNi3MoVA steel, which also indicates that the Ni-MoS<sub>2</sub> coating has better wear resistance than the CrNi3MoVA steel does.

Table 3. Nano-mechanical properties of CrNi3MoVA steel and Ni-MoS<sub>2</sub> coating.

Samples	H (GPa)	E (GPa)	H/E	H <sup>3</sup> /E <sup>2</sup>
CrNi3MoVA steel	4.68	262.8	0.018	0.0015
Ni-MoS <sub>2</sub> coating	5.15	141.5	0.036	0.0068

### 3.3. Friction and wear behavior of CrNi3MoVA steel and Ni-MoS<sub>2</sub> coating

Fig. 5 shows the worn morphologies of the CrNi3MoVA steel (a) and the Ni-MoS<sub>2</sub> coating (b). As shown in Fig. 5, the worn surface of the CrNi3MoVA steel is much rougher than that of the coating. There is a deep furrow on the surface of the CrNi3MoVA steel and two big strips of ploughed adhesion worn debris beside the furrow, which indicating that the dramatic plastic flow occurred on the contacting surface of the CrNi3MoVA steel. Thus the main wear mechanism of the CrNi3MoVA steel can be characterized as adhesive wear. The worn surface of the Ni-MoS<sub>2</sub> coating presents much smoother than the surface of the as-deposited coating. Different from the CrNi3MoVA steel, there are slight scratches and small cracks on the worn surface of the coating. Moreover, under the shear stress effect produced by the reciprocating friction force, some small peeling pits distributed on the surface of the coating. Therefore it suggests that the main mechanism of the coating belongs to abrasive wear and fatigue wear.

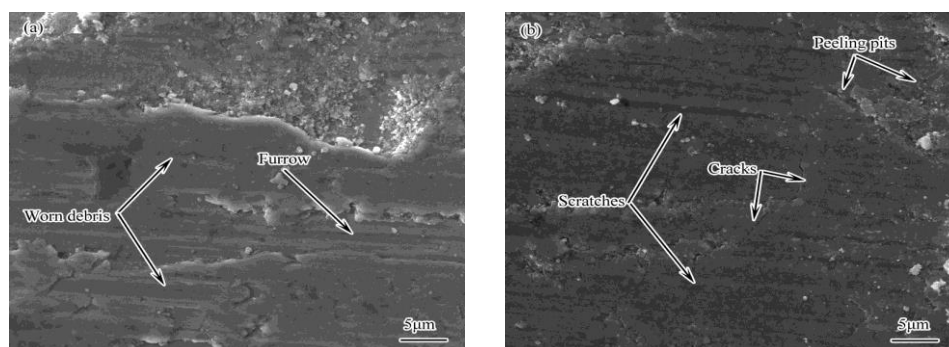


Fig. 5. Worn morphologies of CrNi3MoVA steel (a) and Ni-MoS<sub>2</sub> coating (b).

Fig. 6 shows the friction coefficient (a) and weight loss (b) of the CrNi3MoVA steel and the Ni-MoS<sub>2</sub> coating. As shown in Fig. 6a, the steady friction coefficient of the CrNi3MoVA steel is 0.72-0.78 whilst that of the coating only 0.17-0.20. The friction coefficient of the coating reduced about 75% than that of the CrNi3MoVA steel, so the coating has a remarkable antifriciton effect on the CrNi3MoVA steel. Meanwhile, as shown in Fig. 6b, the weight loss of the CrNi3MoVA steel is 12.17 mg while that of the coating only 2.85 mg, thus the wear resistance of

the coating increased about 77% than that of the CrNi3MoVA steel.

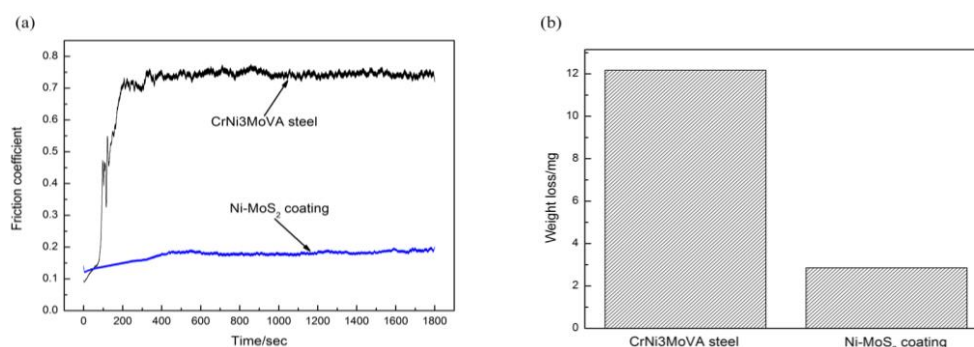


Fig. 6. Friction coefficient (a) and weight loss (b) of CrNi3MoVA steel and Ni-MoS<sub>2</sub> coating.

It is well known that MoS<sub>2</sub> has excellent lubrication property and its friction coefficient is as low as 0.01 in vacuum for the weak Van der Waal's bonding between crystalline layers allows it slide easily. However, in humid atmosphere, MoS<sub>2</sub> shows poor tribological property for it is easily oxidized to MoO<sub>3</sub> leading to an increase of friction coefficient. In the ESD Ni-MoS<sub>2</sub> coating, the MoS<sub>2</sub> particles can be hardly oxidized for they are fully surrounded by  $\gamma$ -Ni, MoO<sub>2</sub> and Ni<sub>x</sub>S, thus the coating maintained a low friction coefficient for a long period. Furthermore, MoS<sub>2</sub> possesses a much stronger adhesion to the Ni matrix than to the steel, which will also increase the wear resistance of the coating [16]. In addition, the Ni-MoS<sub>2</sub> coating prepared by ESD exhibits excellent nano-mechanical properties with higher hardness, H/E value and H<sup>3</sup>/E<sup>2</sup> value, which all favor the increase of the wear resistance.

#### 4. Conclusions

The Ni-MoS<sub>2</sub> coating consists of MoS<sub>2</sub>,  $\gamma$ -Ni, MoO<sub>2</sub> and Ni<sub>x</sub>S for the Ni-MoS<sub>2</sub> electrode reacted with the mixing O<sub>2</sub> in the ESD process. The hardness of the Ni-MoS<sub>2</sub> coating increases about 10.0%, and the elasticity modulus reduces about 46.2% than that of the CrNi3MoVA steel.

The main wear mechanism of the CrNi3MoVA steel can be characterized as adhesive wear whilst that of the Ni-MoS<sub>2</sub> coating belongs to abrasive wear and fatigue wear. The friction coefficient of the Ni-MoS<sub>2</sub> coating reduced about 75%, the wear resistance increased about 77% than that of the CrNi3MoVA steel.

#### Acknowledgment

The authors are grateful for the financial support of the National Science Foundation of Liaoning Province of China (No.201602643 and No.20180550353), and Open Fund of Liaoning Province Armament Science and Technology Key Laboratory of Shenyang Ligong University (No.4771004kfs25).

#### References

- [1] K. P. Furlan, J. D. B. Mello, A. N. Klein, *Tribology International* **120**, 280 (2017).
- [2] J. Wang, M. Chen, Y. Cheng, L. Yang, Z. Bao, L. Liu, S. Zhu, F. Wang, *Corrosion Science* **123**, 27 (2017).
- [3] M. Zhang, M. Shen, L. Xin, X. Ding, S. Zhu, F. Wang, *Corrosion Science* **112**, 36 (2016).
- [4] L. Shi, L. Xin, X. Wang, X. Wang, H. Wei, S. Zhu, F. Wang, *Journal of Alloys and Compounds* **649**, 515 (2015).

- [5] C. Guo, Z. Zhao, F. Lu, B. Zhao, S. Zhao, J. Zhang, Digest Journal of Nanomaterials and Biostructures **13**(4), 931 (2018).
- [6] X. Hong, Y. Tan, C. Zhou, X. Ting, Z. Zhang, Applied Surface Science **356**, 1244 (2015).
- [7] A. E. Kudryashov, D. N. Lebedev, A. Y. Potanin, E. A. Levashov, Surface & Coatings Technology **335**, 104 (2018).
- [8] A. E. Kudryashov, A. Y. Potanin, D. N. Lebedev, I. V. Sukhorukova, D. V. Shtansky, E. A. Levashov, Surface and Coatings Technology **285**, 278 (2015).
- [9] T. Cao, S. Lei, M. Zhang, Surface and Coatings Technology **270**, 24 (2015).
- [10] J. Yang, Y. Wang, J. Qu, Q. Guo, H. Jin, C. Guo, J. Zhang, Materials Review **31**(1), 51 (2017).
- [11] Y. J. Liang, Y. C. Che, Handbook of Inorganic Compound of Thermodynamic Data, 1<sup>nd</sup> ed., Northeastern University, Shenyang 1993, 239.
- [12] X. F. Lu, H. M. Wang, Materials Characterization **60**, 834 (2009).
- [13] X. Wang, Z. Wang, P. He, T. Lin, Y. Shi, Surface & Coatings Technology **283**, 156 (2015).
- [14] A. Leyland, A. Matthews, Wear **246**(1), 1 (2000).
- [15] L. Ipaz, J. C. Caicedo, J. Esteve, F. J. Espinoza-beltran, G. Zambrano, Applied Surface Science **258**(8), 3805 (2012).
- [16] Y. He, S. Wang, F. C. Walsh, Y. L. Chiu, P. A. S. Reed, Surface & Coatings Technology **307**, 926 (2016).